Characterization of Water Vapor Permeable Membranes

Akshaya Jena and Krishna Gupta
Porous Materials, Inc., 83 Brown Road, Ithaca, NY 14850, USA, Phone: (607) 257-5544,
Fax: (607) 257-5639, info@pmiapp.com

Abstract

Air permeability and water vapor permeability of nafion membranes were measured using specially built instruments. Air permeability was almost zero. Water vapor permeability was zero during an incubation period. After the incubation period, the permeability became large and then gradually decreased with time. The behavior has been attributed to the contributions of chemical and mechanical forces to the net flux through the membrane. A model consistent with these results has been presented to explain absorption and transport of water vapor through nafion membranes.
Keywords: Nafion Membrane. Vapor Permeation. Air Permeation.

Introduction

Many novel membranes with unusual characteristics are currently being manufactured to meet the growing demands of modern technology. A number of membranes are almost completely impermeable to air but are permeable to water vapor. Nafion is one such commercial membrane. Membranes, which do not permit air to pass through them, but permit passage of water vapor, find important applications in power source, pharmaceutical and biotech industries. It is not possible to characterize such materials using the available techniques. Special techniques are needed to characterize the unique properties of such membranes. Novel techniques were developed to characterize some of these unusual properties. Permeation rates through commercial nafion membranes were measured using these techniques. Water vapor transmission rates through nafion membranes were also measured. The paper describes the equipment and its performance and critically evaluates the results.

Technique

Gas Transmission Rate

The sketch in Figures 1 illustrates the principles of the instrument developed to investigate the permeability of nearly impermeable membranes. The sample is loaded in the sample chamber and the instrument is evacuated. Gas is introduced on one side of the sample chamber and the pressure of the gas is maintained at a constant value. The increase in pressure on the other side of the sample is accurately measured. In order to obtain the utmost accuracy, the system is maintained at a constant temperature. Flow rates through the sample are computed from the rates of pressure increase.

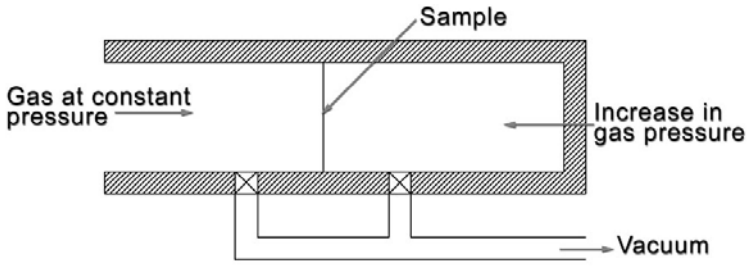

Figure 1. Principle of diffusion permeameter.

The instrument, Diffusion Permeameter was designed based on this principle. It is shown in Figures 2. The instrument is completely automated and requires very little operator involvement. Windows based software is used for ease of operation, data acquisition and data reduction. The instrument is capable of accurately measuring very small increments in pressure so that, flow rates as low as 10^{-4} cm^3/s can be detected.

Figure 2. The PMI Diffusion Permeameter.

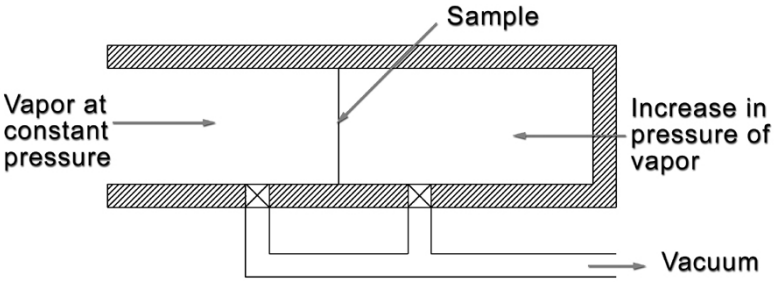

Figure 3. Principle of water vapor transmission analyzer.

Water Vapor Transmission Rate

The principle of water vapor transmission analyzer is illustrated in Figure 3. The system is evacuated after placing the sample in the sample chamber. Water vapor is brought in to the sample chamber on one side of the sample and the pressure of the vapor is maintained at a constant value. The increase in pressure of the water vapor on the other side of the sample is continuously monitored. The vapor transmission rates are calculated from the measured values of pressure.

The Water Vapor Transmission Analyzer was designed based on this principle. It is similar to the diffusion permeameter shown in Figure 3. The instrument is completely automated and the results are highly reproducible, accurate and objective. Use of windows based software makes operation, data acquisition and data reduction simple and operator involvement minimal. The instrument is capable of accurately measuring very small increments in pressure so that, very low flow rates could be detected.

Results and Discussion

Material

The newly developed commercial nafion membranes were procured and investigated using the diffusion permeameter and the water vapor analyzer.

Gas Permeation

Samples of the membrane were investigated in the diffusion Permeameter. The pressure rise on the outlet side of samples of two 0membranes was measured. The data presented in Figure 4 demonstrate that the instrument was sensitive enough to measure the small increments in pressure. The rate of pressure increase is related to the volume flow rate.

$$(dV_s / dt) = (T_s V_o / T p_s) (dp / dt) \quad (1)$$

where V_s is the gas flow rate in volume of gas referred to standard pressure, p_s and standard temperature T_s; t is time; V_o is volume of chamber on the outlet side; T is test temperature; and p is pressure on the outlet side of the sample chamber. The data in Figure 4 show constant flow rates. The flow rate through the membranes is less than 0.75×10^{-4} cm^3/s. Thus, the pressure increments correspond to almost negligible flow rates of gas through the membrane and the membrane is almost impermeable to gas.

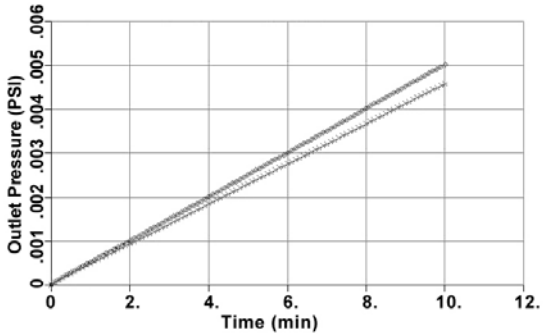

Figure 4. Change of outlet gas pressure with time for two samples measured in the Diffusion Permeameter.

Water Vapor Transmission Rate

The same membranes were investigated in the PMI Water Vapor Transmission Analyzer. The pressure rise of water vapor on the outlet side of two samples is shown in Figure 5. The pressure rise on the outlet side is almost twenty times the pressure rise observed in the diffusion permeameter. Thus, the water vapor permeation rate through the nafion membrane is appreciable although the air permeation rate is negligible.

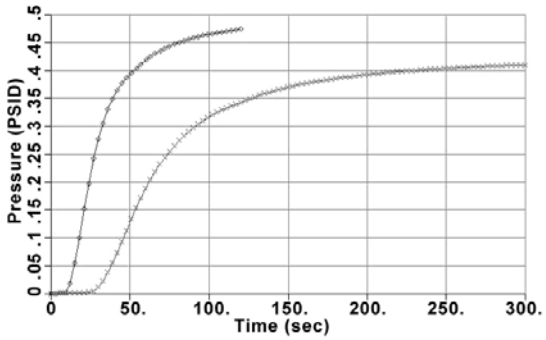

Figure 5. Change of pressure on the outlet side of two samples of the membrane in the PMI Water Vapor Transmission Analyzer

The variation of pressure with time is sigmoidal. An incubation period is observed at the beginning. During the incubation period the pressure does not increase on the outlet side of the sample. After the incubation period, the pressure increases at first with increasing rate in a short transition zone and then with decreasing rate and approaches the constant inlet pressure of the vapor.

Permeability

The increase of pressure on the outlet side is due to transfer of water vapor through the sample to the outlet side. The molar rate of vapor transfer through the sample may be written as [1]:

$$dn/dt = - K (dp/dl) \quad (2)$$

where n is the moles of vapor transferred through unit area of the sample in time, t; (dp/dl) is the pressure gradient across the thickness of the sample; and K is the permeability in moles per unit area, unit time and unit pressure gradient. In terms of the constant inlet pressure p_0, outlet pressure p_i and thickness of the sample l_0:

$$dn/dt = K [(p_0 - p_i) / l_0] \quad (3)$$

The rate of pressure increase in the sample chamber is given by:

$$dp_i/dt = (RT/V_0) (dn_c/dt) \quad (4)$$

where R is the gas constant, T is the test temperature, V_0 is the volume of chamber on the outlet side of sample, n_c is the moles of water vapor in the chamber. (dn_c/dt) is equal to the rate of transfer, (dn/dt) of Equation 3 times the surface area A of the sample. Substituting from Equation 3:

$$dp_i/dt = (RTAK / V_0 l_0) (p_0 - p_i) \quad (5)$$

On integration:

$$\ln (p_0 - p_i) = - (RTAK / V_0 l_0) t + c \quad (6)$$

where c is a constant. This relation shows that the plot of $\ln (p_0 - p_i)$ versus t should have a slope equal to the negative of ($RTAK / V_0 l_0$), which is a measure of water vapor permeability through the membrane.

The plot of $\ln (p_0 - p_i)$ against time is shown in Figure 6. Initially the slope is zero as there is no transfer of vapor through the sample during the incubation period. After the incubation period, the rate of transfer becomes appreciable as demonstrated by the appreciable negative slope of the curve.

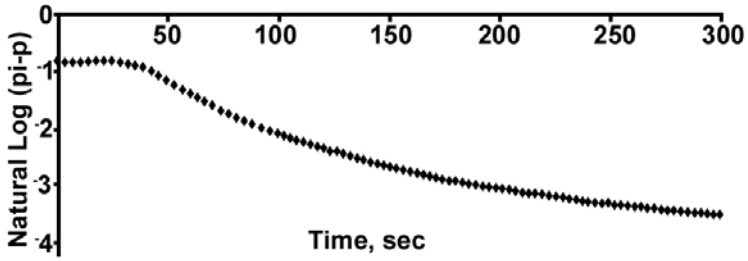

Figure 6. Variation of $\ln (p_0 - p_i)$ with time.

The permeability does not remain constant. It decreases with increase in time. A plot of negative of slope, [-d $\ln (p_o-p_i)$ / dt] versus time is presented in Figure 7. It shows that permeability is zero in the incubation period. The permeability increases quickly to a high value in the transition zone and then decreases appreciably.

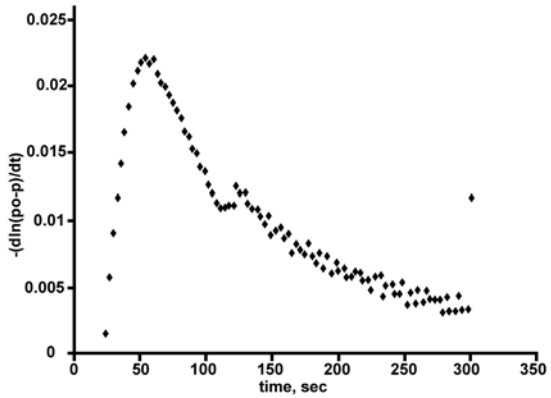

Figure 7 Variation of the slope of the curve in Figure 6 with time.

Mechanism

The proposed mechanism envisages that the side of the membrane that comes in contact with vapor develops a surface concentration in equilibrium with the vapor. With increase in time, the migration of water vapor occurs along the thickness direction of the membrane. When the concentration on the far side of the membrane becomes greater than zero, vapor at a pressure in equilibrium with the concentration on the far side is created. The schematic variation of concentration along the depth as a function of time is illustrated in Figure 8.

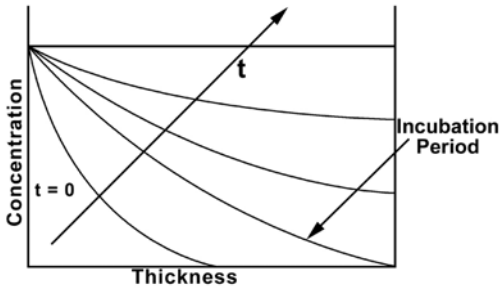

Figure 8 Schematic variation of the moisture concentration in membrane with time.

The dry membrane is impervious to air. It is also expected to be impervious to the large molecules of water vapor. However, when the membrane is exposed to water vapor, the membrane chemically attracts the vapor and absorbs the vapor. The part of the membrane that absorbs water vapor becomes conducting to the vapor, but rest of the membrane remains dry and non-conducting. Therefore, vapor transport through the membrane is zero in the initial stages until the moisture concentration on the far side of the membrane becomes greater than zero. The result is the incubation period (Figure 8).

After the incubation period, the material flux through the membrane is given by the sum of contributions by two forces [2]. The mechanical force due to pressure gradient and the chemical force due to interaction of water vapor with membrane. The flux due to mechanical force is proportional to pressure gradient while that due to chemical force is proportional to concentration gradient.

$$J = K_1 [(C_0 - C_i) / l_0] + K_2 [(p_0 - p_i) / l_0] \quad (7)$$

where J is the net flux per unit area and unit time, C is the concentration, K_1 and K_2 are constants. Permeability is defined as the net flux per unit pressure gradient. Hence:

$$K = J / [(p_0 - p_i) / l_0] = K_1 [(C_0 - C_i) / (p_0 - p_i)] + K_m \quad (8)$$

where K_m, the contribution to permeability from mechanical force, is the same as K_2.

The relation between C and p is determined by the chemical absorption reaction that takes place between the membrane and water vapor. It is improbable that large water molecules can move freely in the membrane. Many gases are known to be present in liquids as atoms. The water molecule is likely to decompose into its component atoms for absorption by the membrane as represented by the following reaction [3].

$$H_2O\ (g) \Leftrightarrow 2H(m) + O(m)$$

Noting that twice the concentration of O, 2C(O), is equal to the concentration of H, C(H), the equilibrium constant, K_{eq} for this reaction is given by:

$$K_{eq} = C^2(H)\, C(O) / p_{H2O} = 4C^3(O) / p_{H2O} \quad (9)$$

Consequently:

$$C(O) = [(1/4)\, K_{eq}]^{1/3} [p_{H2O}]^{1/3} \quad (10)$$

Expressing concentration in terms of pressure after Equation 10, Equation 8 reduces to:

$$K = [K_c / f(p)] + K_m \quad (11)$$

Where:

$$f(p) = [\, p_0^{2/3} + p_i^{2/3} + p_0^{1/3} p_i^{1/3}] \quad (12)$$

and K_c determines the chemical contribution to permeability. The pressure term on the denominator of the first term on the right of the equation is smallest at the beginning and largest at the end. Therefore, the chemical contribution to permeability is large at the beginning and small at the end.

Experimental values of K taken from Figure 7 are plotted in Figure 9 against f(p) after Equation 11. When p_i is zero, [1/f(p)] has the highest value, K_m is zero and the slope of the curve in Figure 9 is equal to K_c. With increase in pressure, [1/f(p)] decreases and the slope of the plot in Figure 9 increases. The increasing slope suggests increasing contribution of mechanical force to permeability with increase in pressure. Thus, the contribution of mechanical force to permeability increases with increase in pressure, while the contribution of chemical force to permeability decreases with increasing pressure.

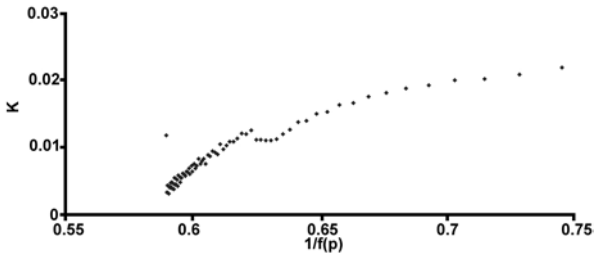

Figure 9. Plot of K versus [1/f(p)] where $f(p) = [p_0^{2/3} + p_i^{2/3} + p_0^{1/3} p_i^{1/3}]$.

The contributions of the two forces to permeability are schematically illustrated in Figure 10. The net change is a reduction in permeability with time. The data in Figure 7 demonstrate such behavior. All the experimental results are consistent with the proposed model for absorption and transmission of the water vapor through nafion membranes.

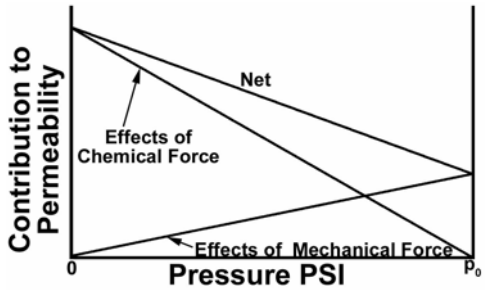

Figure 10. Schematic effect of chemical and mechanical forces on permeability.

Conclusions

Instruments capable of accurately measuring very small gas permeability and water vapor permeability have been described and used to investigate nafion membranes. Nafion membranes show negligible air permeability. The permeability of water vapor is appreciable after an initial incubation period in which the permeability is zero. The large permeability observed after the incubation period gradually decreases with time. It is proposed that the vapor maintains an equilibrium solute concentration on one side of the membrane. The solute gradually migrates to the other side. The incubation period is observed until the concentration on the far side of the membrane reaches a non-zero value. Beyond the incubation period, the flux of solutes has contributions from the chemical force due to chemical interaction of water with the membrane and the mechanical force due to pressure gradient. The chemical permeability is large at the beginning, but small at the end. On the other hand, mechanical permeability is smaller at the beginning.

References

1. S. Lowell and E. Shields, Powder Surface Area and Porosity, Chapman and Hall. 1984.
2. W. Jost, Diffusion, Academic Press, 1951.
3. K. Denbigh, The Principles of Chemical Equilibrium, Cambridge University Press, 1968.